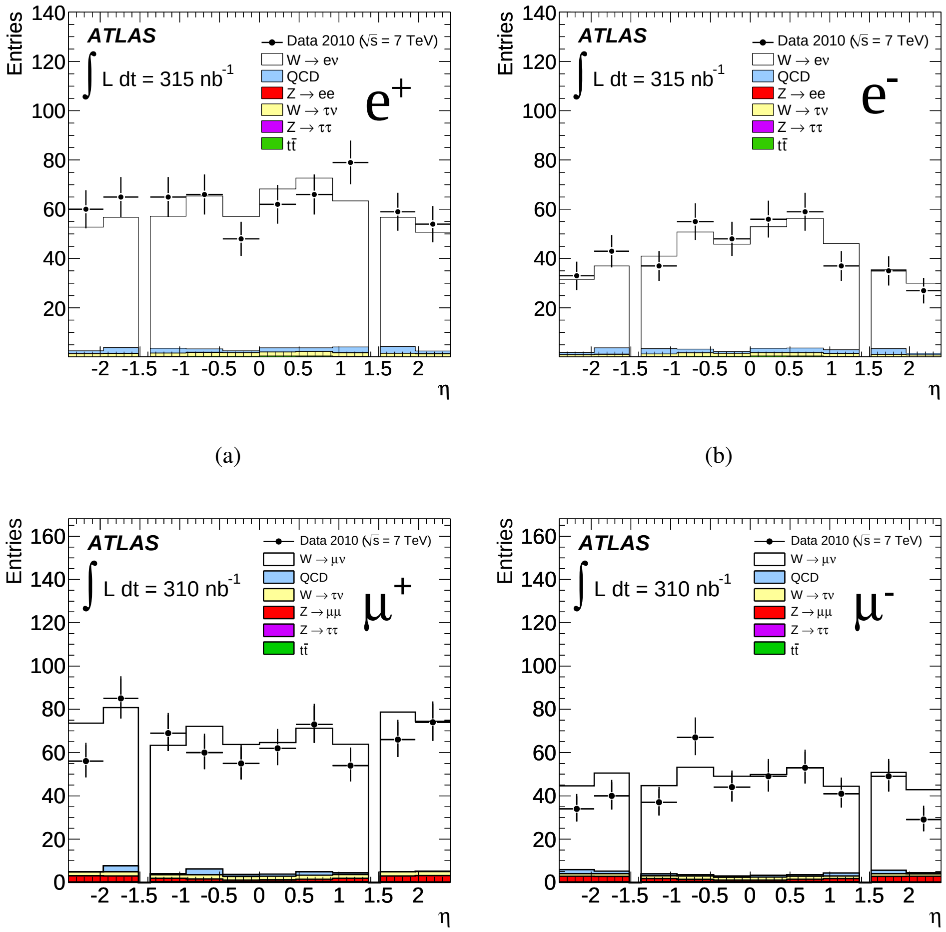

(a) (b) (c) (d)

Fig. 15: *Pseudorapidity distributions of e^+ (a), e^- (b), μ^+ (c) and μ^- (d) candidates satisfying all W requirements (see Section 5.4). The data are compared to the Monte Carlo simulation, broken down into the signal and various background components. The Monte-Carlo distributions are normalised to the integrated luminosity of the data, as described in Section 5.2.*

η range	Electron channel A_e	Muon channel A_μ	Combination A_ℓ
$\lvert\eta\rvert < 1.37$	$0.15 \pm 0.04 \pm 0.00$	$0.12 \pm 0.04 \pm 0.01$	$0.14 \pm 0.03 \pm 0.01$
$1.52 < \lvert\eta\rvert < 2.4$	$0.29 \pm 0.05 \pm 0.02$	$0.32 \pm 0.05 \pm 0.02$	$0.31 \pm 0.04 \pm 0.01$
$\lvert\eta\rvert < 1.37$ and $1.52 < \lvert\eta\rvert < 2.4$	$0.21 \pm 0.03 \pm 0.01$	$0.19 \pm 0.03 \pm 0.01$	$0.20 \pm 0.02 \pm 0.01$

Table 15: The measured lepton asymmetries integrated over the full pseudorapidity range, as well as separately for the barrel and end-cap regions. The quoted uncertainties are statistical (first) and systematic (second).

For the muon channel, the systematic uncertainty is derived from uncertainties on the muon momentum scale and resolution ($\pm 5.0\%$), from uncertainties on the trigger efficiency ($\pm 2.7\%$), and on the QCD ($\pm 0.8\%$) and electroweak backgrounds ($\pm 0.5\%$). The muon momentum scale and resolution may depend significantly on charge. Scale and resolution uncertainties on the muon momentum measurement are considered to be anti-correlated, since they could affect in opposite directions the bending of tracks of opposite sign.

The measured lepton asymmetries are displayed in Fig. 16 as a function of $|\eta|$ and compared to theo-